Journal of Ginseng Research 48 (2024) 52–58

Contents lists available at ScienceDirect

Journal of Ginseng Research

journal homepage: www.sciencedirect.com/journal/journal-of-ginseng-research

Research Article

Korean red ginseng suppresses mitochondrial apoptotic pathway in denervation-induced skeletal muscle atrophy

Ji-Soo Jeong, Jeong-Won Kim, Jin-Hwa Kim, Chang-Yeop Kim, Je-Won Ko**, Tae-Won Kim*

College of Veterinary Medicine (BK21 FOUR Program), Chungnam National University, Daejeon, Republic of Korea

ARTICLE INFO

Article history:
Received 13 December 2022
Received in revised form
8 June 2023
Accepted 1 July 2023
Available online 5 July 2023

Keywords:
Korean red ginseng
denervation
mitochondria-activated apoptosis
myogenesis

ABSTRACT

Background: Skeletal muscle denervation leads to motor neuron degeneration, which in turn reduces muscle fiber volumes. Recent studies have revealed that apoptosis plays a role in regulating denervation-associated pathologic muscle wasting. Korean red ginseng (KRG) has various biological activities and is currently widely consumed as a medicinal product worldwide. Among them, ginseng has protective effects against muscle atrophy in *in vivo* and *in vitro*. However, the effects of KRG on denervation-induced muscle damage have not been fully elucidated.

Methods: We induced skeletal muscle atrophy in mice by dissecting the sciatic nerves, administered KRG, and then analyzed the muscles. KRG was administered to the mice once daily for 3 weeks at 100 and 400 mg/kg/day doses after operation.

Results: KRG treatment significantly increased skeletal muscle weight and tibialis anterior (TA) muscle fiber volume in injured areas and reduced histological alterations in TA muscle. In addition, KRG treatment reduced denervation-induced apoptotic changes in TA muscle. KRG attenuated p53/Bax/cytochrome c/Caspase 3 signaling induced by nerve injury in a dose-dependent manner. Also, KRG decreases protein kinase B/mammalian target of rapamycin pathway, reducing restorative myogenesis.

Conclusion: Thus, KRG has potential protective role against denervation-induced muscle atrophy. The effect of KRG treatment was accompanied by reduced levels of mitochondria-associated apoptosis.

1. Introduction

Skeletal muscle atrophy is characterized by decreasing muscle volume that leads to muscle weakness and disability. It is caused by aging, immobility, medication, or a wide spectrum of injuries or diseases that affect the nervous or musculoskeletal system [1]. Motor innervation is an important regulator of skeletal muscle mass and function [2,3]. Nerve injury activates numerous well-known proteolytic pathways that increase the rate of protein degradation. A concurrent decrease in the rate of protein synthesis results in a marked reduction in muscle fiber size [4].

In addition to these pathways, apoptosis has recently been shown to be an important contributor to the atrophic response associated with chronic muscle disuse and pathological muscular diseases [5,6], shown by a decline in the mitochondrial content per gram of muscle mass. This reduction suggests that chronic inactivity may induce adaptations to the mitochondria, making them sensitive to the release of apoptotic proteins [7]. Previous studies illustrated the activation of mitochondria-associated apoptotic signaling in denervation-induced skeletal muscle atrophy. Levels of the transcription factor p53, a regulator of mitochondrial quality and function in muscle, increased following denervation, along with a concomitant increase in the level of pro-apoptotic Bax, a p53-regulated protein [8]. In addition, denervated muscle contains increased levels of Bax, mitochondrial release of cytochrome c, and activation of Caspase 3, recognized as key regulators of cell death [9].

Panax ginseng Meyer is an oriental herbal medicine that is now extensively consumed as a medicinal product worldwide [10].

Abbreviations: AKT, protein kinase B; DAB, 3,3-diaminobenzidine; GA, gastrocnemius; IHC, immunohistochemistry; KRG, Korean red ginseng; m-TOR, mammalian target of rapamycin; p.o., per oral administration; SD, standard deviations; TA, tibialis anterior.

* Corresponding author. College of Veterinary Medicine (BK21 FOUR Program), Chungnam National University, 99 Daehak-ro, Daejeon, 34131, Republic of Korea.
** Corresponding author. College of Veterinary Medicine (BK21 FOUR Program), Chungnam National University, 99 Daehak-ro, Daejeon, 34131, Republic of Korea.
E-mail addresses: rheoda@cnu.ac.kr (J.-W. Ko), taewonkim@cnu.ac.kr (T.-W. Kim).

https://doi.org/10.1016/j.jgr.2023.07.002

Korean red ginseng (KRG) possesses multiple biological activities, including antioxidant, anti-inflammatory, and antitumor effects [11]. The active components of KRG are ginsenosides, which are triterpene glycosides [12]. Ginsenosides exert medicinal effects via their anti-apoptotic effects on various cells [13–15]. Ginsenosides can block Bax/Caspase 3 release and protect against mitochondria-activated cell apoptosis [16]. In addition, ginseng has protective effects against muscle atrophy in *in vivo* and *in vitro* [17,18]. Ginsenoside Rg1 reported to prevent muscle protein degradation and atrophy in C2C12 myotubes [19]. Although KRG has been confirmed to have anti-apoptotic and protective effects against muscle atrophy [14,18], the effects of KRG on denervation-induced muscle damage have not been fully elucidated.

The aim of this study was to evaluate the ability of KRG to prevent denervation-induced skeletal muscle atrophy. We investigated the effects of KRG on the extent of apoptosis and myogenesis in denervation-related muscle atrophy.

2. Materials and methods

2.1. Animals and experimental groups

Six-week-old male C57BL/6 mice (20–23 g, Orient Bio Inc., Seongnam, Korea) were housed under standard conditions (temperature, 22 ± 3 °C; humidity, 23 ± 5 °C; 12 h light/dark cycles) with water and food ad libitum. After 1 week of acclimation, mice were randomly divided into four groups ($n = 7$ mice/group): (1) Sham, (2) Denervation, (3) Denervation + oral administration of low-dose KRG (100 mg/kg), and (4) Denervation + oral administration of high-dose KRG (400 mg/kg). KRG (Hong Sam Jung; lot no. H2006(2) 1043) was purchased from the Korea Ginseng Corporation (Daejeon, Republic of Korea). The major ginsenosides, Rb1 (6 mg/g), Rd (1 mg/g), and Rg3 (1.5 mg/g), were confirmed by HPLC analysis, previously described by Kim et al, 2022 [20]. Animal care and experimental procedures followed the Animal Care and Use Committee of Chungnam National University (202112A-CNU-194) guideline.

2.2. Denervation procedures and animal treatment

The mouse's right hind leg sciatic nerve was transected to construct a mouse model of muscle atrophy *in vivo*. All mice were anesthetized, and the right hind legs were shaved to prepare a surgical window. After femoral palpation, the incision line was placed adjacent to the middle of the femur, and the muscle fibers were carefully separated by retracting the scissors until the sciatic nerve was identified. The sciatic nerve was dissected, and the skin was sutured cautiously to avoid damage to other muscle fibers. KRG dosages were selected based on a previous study [20] and administered by oral gavage once a day for 3 weeks at 100 and 400 mg/kg/day postoperatively. Body weight was measured weekly during the treatment. Mice were sacrificed by carbon dioxide one day after the last KRG treatment. Tibialis anterior (TA), gastrocnemius (GA), and quadriceps were harvested for Western blot and histological analysis.

2.3. Histological analysis

Formalin-fixed TA muscle tissue was embedded in paraffin, and sectioned into 4 μm-thick slices. After deparaffinization and rehydration, all sections were stained with Harris' hematoxylin and eosin (TissuePro Technology, Gainesville, FL) for light microscopic observation (Leica, Wetzlar, Germany). All slides were scanned using a digital slide scanner (MoticEasyScan Oro, Motic, Xiamen, China). Randomly selected areas from each slide were captured using Motic Digital Slide Assistant software (Version 1.0.7.44, Motic).

2.4. Immunofluorescence staining

TA muscles were fixed in 4% (v/v) paraformaldehyde and permeabilized with 0.2% Triton X-100 in phosphate-buffered saline to determine the skeletal muscle fibers' cross-sectional areas. The muscles were incubated sequentially with an anti-laminin primary antibody (1:50, Abcam, Cambridge, MA, USA) and goat anti-rabbit Alexa Flour 488 conjugated secondary antibody (1:500, Abcam), protected from light. The sections were individually mounted in DAPI (Abcam) and sealed with a coverslip. The specimens were analyzed using a confocal laser-scanning microscope (Nikon Corporation, Tokyo, Japan). DAPI (blue) and laminin (green) fluorescence were excited with a 405 nm and a 488 nm, respectively.

2.5. Terminal deoxynucleotidyl transferase dUTP nick end labeling (TUNEL) assay

TUNEL assay (Abcam) was used to measure apoptotic cell death in the control and experimental groups. Apoptotic cell death was visualized using 3,3-diaminobenzidine (DAB) chromogen with a Harris's hematoxylin counterstain for microscopic examination (Leica). IMT i-Solution software was used for quantitative image analysis.

2.6. Immunohistochemistry (IHC) analysis

Myogenin expression was visualized using a VECTASTAIN Elite ABC kit (Vector Laboratories, Burlingame, CA, USA), based on the manufacturer's protocol. After deparaffinization and dehydration, the sections were treated with citric buffer for antigen retrieval. After serial washing, endogenous peroxidase quenching and blocking was followed. After blocking all sections were incubated with anti-myogenin (1:500, Abcam) and goat anti-rabbit IgG primary and secondary antibodies, respectively. DAB chromogen and Harris hematoxylin were used for color development. All the sections were randomly evaluated using a light microscope (Leica).

2.7. Immunoblotting

Frozen muscle tissue was homogenized with a tissue lysis buffer (Sigma-Aldrich, St. Louis, MO, USA) with a protease inhibitor cocktail (Sigma-Aldrich) and a phosphatase inhibitor cocktail (Sigma-Aldrich). The suspension was centrifuged at 12,000 g at 4 °C for 15 min to isolate the cellular proteins in the supernatant. Western blot analysis was performed according to a previous study [21]. After blocking with bovine serum albumin, the membranes were incubated with the following primary antibodies and dilutions: total (t)-p53 (1:1000, Abcam), phosphor (p)-p53 (1:1000, Cell Signaling Technology, Beverly, MA, USA), Bax (1:1000, Abcam), cytochrome c (1:1000, Abcam), Caspase-3 (1:1000, Cell Signaling Technology), t-protein kinase B (t-AKT, 1:1000, Abcam), p-AKT (1:1000, Abcam), t-mammalian target of rapamycin (t-mTOR, 1:1000, GeneTex, Irvine, CA, USA), p-mTOR (1:1000, GeneTex), and myogenin (1:1000, Abcam). Ponceau S staining was used as a loading control in Western blot analysis [22,23]. Each protein band was quantitated by ChemiDoc imaging system (Bio-Rad Laboratories, Hercules, CA, USA).

2.8. Statistical analysis

All data are expressed as mean ± standard deviation (SD). Means of more than two groups were analyzed by using one-way analysis of variance (ANOVA) followed by Tukey's honestly significant difference test. Statistical significance was determined by comparing the treatment groups to the sham group using GraphPad InStat v. 3.0 (GraphPad Inc., La Jolla, CA, USA). Statistical significance was set at p value less than 0.05 and 0.01 were considered significant.

3. Results

3.1. Effects of KRG on denervation-induced muscle wasting

When body weight was measured weekly for KRG treatment after surgery, no significant change in body weight was observed in any group (Table 1). However, sciatic nerve injury causes a reduction in neural innervation of the TA muscle, leading to reduced muscle weight. The reduction was quantified by measuring the muscles weight from the operated group and normalizing to body weight. In the denervation group, the weight of the right TA muscle was evidently lower than that in the sham group. In contrast, the KRG treatment groups showed a dose-dependent decrease in TA muscle weight compared to the denervation group.

Additionally, muscle weight loss in the denervation group was observed in the GA muscles. However, no significant difference was detected in GA. There was no change in muscle mass after denervation or KRG treatment in the quadriceps. Morphological atrophy of TA muscles due to denervation and recovery due to KRG administration were observed visually (Fig. 1).

3.2. Effects of KRG on denervation-induced histological alterations in the TA muscle

The protective effects of KRG against nerve damage were also observed in the histological results (Fig. 2A and B). The sham group showed intact TA muscle. In contrast, the denervation group showed atrophied muscle fibers and a disorganized morphology and structure. The nuclei were enlarged and abnormally located (arrowheads). These pathological changes were improved by KRG treatment in a dose-dependent manner (Fig. 2A).

The immunofluorescence results showed that muscle fiber areas were markedly reduced in denervated muscles (Fig. 2B), indicating that the denervated muscle atrophy mouse model has been established. However, muscle fiber areas increased with the increasing KRG concentration in the treated damaged TA muscle. These results suggest that KRG may promote the recovery of TA muscle innervation.

Table 1
KRG on Body Weight and Muscle Weight in Denervation-induced mice

Group	SHAM	DEN	DEN + KRG L	DEN + KRG H
Body weight (g)				
Before surgery	20.65 ± 1.17	21.37 ± 1.02	21.35 ± 0.61	22.07 ± 0.86
1 week	21.38 ± 1.18	21.22 ± 0.90$^{\#\#}$	21.25 ± 0.52**	21.82 ± 0.91**
2 weeks	21.75 ± 0.79	22.04 ± 1.25	21.23 ± 0.48	21.75 ± 0.78
3 weeks	24.13 ± 1.54	23.85 ± 1.24	21.53 ± 1.32**	23.20 ± 0.69
4 weeks	23.8 ± 1.26	23.44 ± 1.15	22.03 ± 1.38	23.00 ± 0.91
Muscle weight / Body weight (%)				
Quadriceps	0.717 ± 0.170	0.699 ± 0.111	0.794 ± 0.068	0.795 ± 0.020
Tibialis anterior	0.142 ± 0.050	0.087 ± 0.003$^{\#\#}$	0.109 ± 0.019**	0.117 ± 0.023**
Gastrocnemius	0.440 ± 0.123	0.285 ± 0.049	0.253 ± 0.088	0.279 ± 0.009

Values: means ± SD (n = 7). Significance: $^{\#\#}p < 0.01$ vs SHAM; $^{**}p < 0.01$ vs DEN.

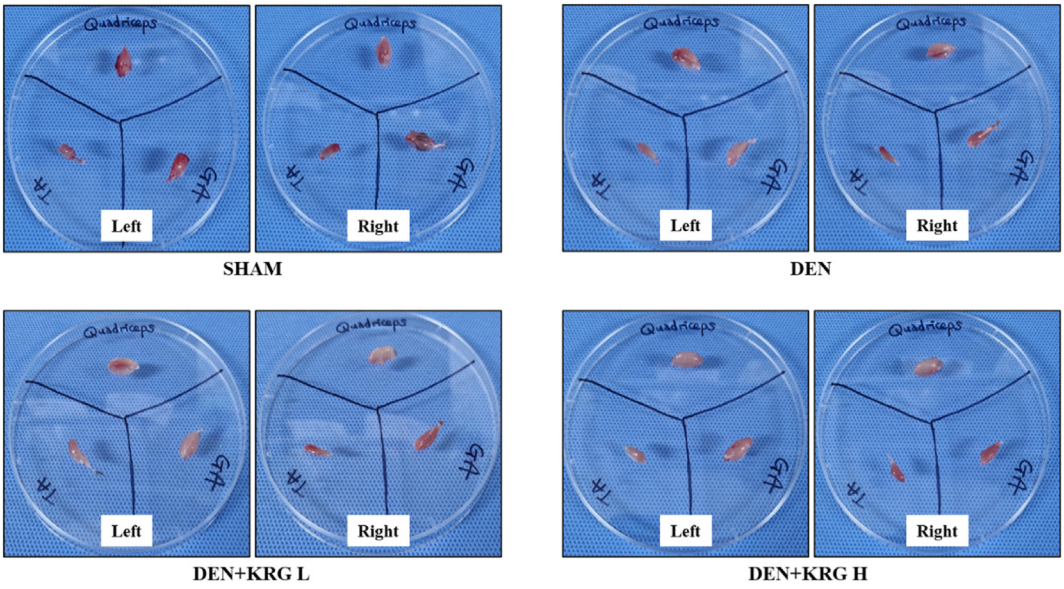

Fig. 1. Representative photographs of TA, GA, and quadriceps in denervation-induced mice. Nerve dissected muscles are on the right, and contralateral muscles are on the left. DEN; denervation-induced mice, DEN + KRG L; denervation-induced mice + oral administration of low-dose (100 mg/kg/day) of KRG, DEN + KRG H; denervation-induced mice + oral administration of high-dose (400 mg/kg/day) KRG.

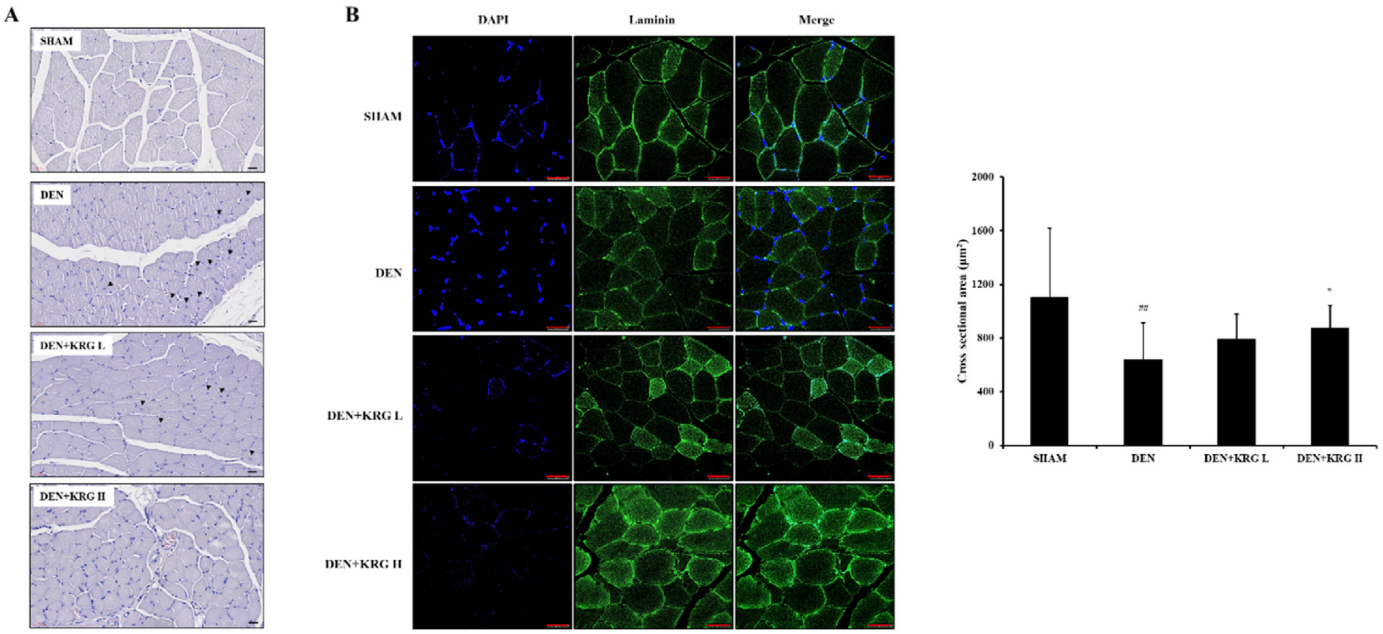

Fig. 2. KRG improves the histological alterations and the atrophied muscle fibers size in TA muscles from mice which was confirmed by (A) Harris' hematoxylin and eosin staining (Bar = 30 μm) and (B) immunofluorescence laminin staining (Bar = 25 μm). The nuclei were enlarged and abnormally located (arrowheads). DEN; denervation-induced mice, DEN + KRG L; denervation-induced mice + oral administration of low-dose (100 mg/kg/day) of KRG, DEN + KRG H; denervation-induced mice + oral administration of high-dose (400 mg/kg/day) KRG. Values: means ± SD ($n = 7$). Significance: $^{\#\#}p < 0.01$ vs SHAM; $^{*}p < 0.05$ vs DEN, respectively.

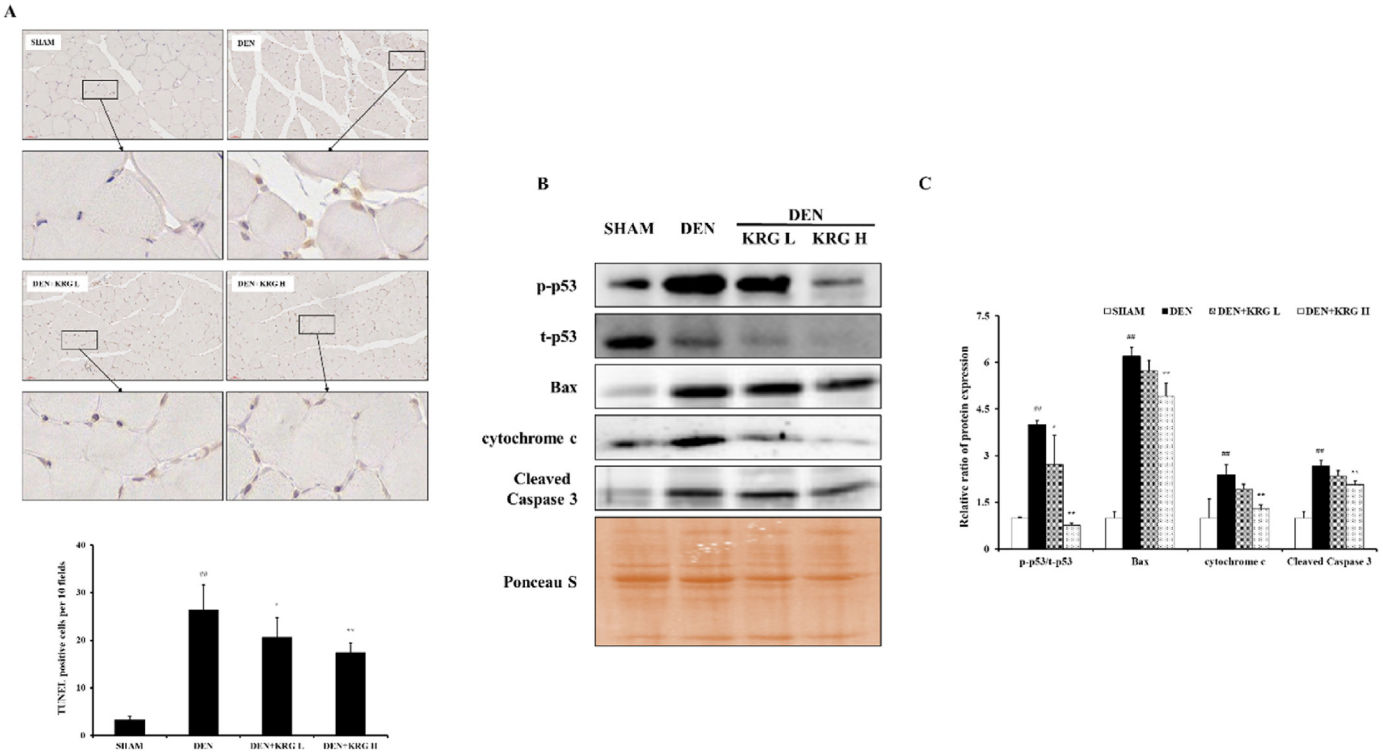

Fig. 3. KRG reduces the elevated apoptosis in TA muscles (A) and suppresses the elevated pro-apoptotic signals (B). (C) The densitometric values were determined using ChemiDoc. DEN; denervation-induced mice, DEN + KRG L; denervation-induced mice + oral administration of low-dose (100 mg/kg/day) of KRG, DEN + KRG H; denervation-induced mice + oral administration of high-dose (400 mg/kg/day) KRG. Values: means ± SD ($n = 7$). Significance: $^{\#\#}p < 0.01$ vs SHAM; $^{*,**}p < 0.05$ and 0.01 vs DEN, respectively.

3.3. Effects of KRG on denervation-induced apoptosis in the TA muscle

We used a TUNEL assay to observe the effects of KRG on apoptotic changes caused by denervation in the TA muscle tissue (Fig. 3A). A section of the TA muscle shows that the number of TUNEL-positive cells was higher in the denervation-alone treated group than that from the sham group. In contrast, the denervation + KRG-treated groups showed fewer TUNEL-positive cells, in a dose-dependent pattern, compared to the denervation-alone treated group.

We performed Western blot on p53/Bax/cytochrome c/Caspase 3 (Fig. 3B). Compared to the sham group, the denervation group showed increased expression levels of p53/Bax/cytochrome c/Caspase 3. In contrast, denervation-induced, mitochondria-mediated apoptosis-related signaling proteins were significantly suppressed in the KRG-treated groups. However, the effects of KRG treatment on denervation-induced Caspase 3 expression in the GA and quadriceps showed no difference when compared to that from the denervation-alone treated group (Supplemental Fig. 1).

3.4. Effects of KRG on the denervation-induced proliferation-related signal in the TA muscle

The effects of KRG on proliferation-related signals in denervated muscles were explored by assessing AKT and mTOR phosphorylation levels. Denervation increased the phosphorylation of AKT and mTOR to repair damaged TA muscles (Fig. 4). However, KRG treatment groups showed a concentration-dependent decreased

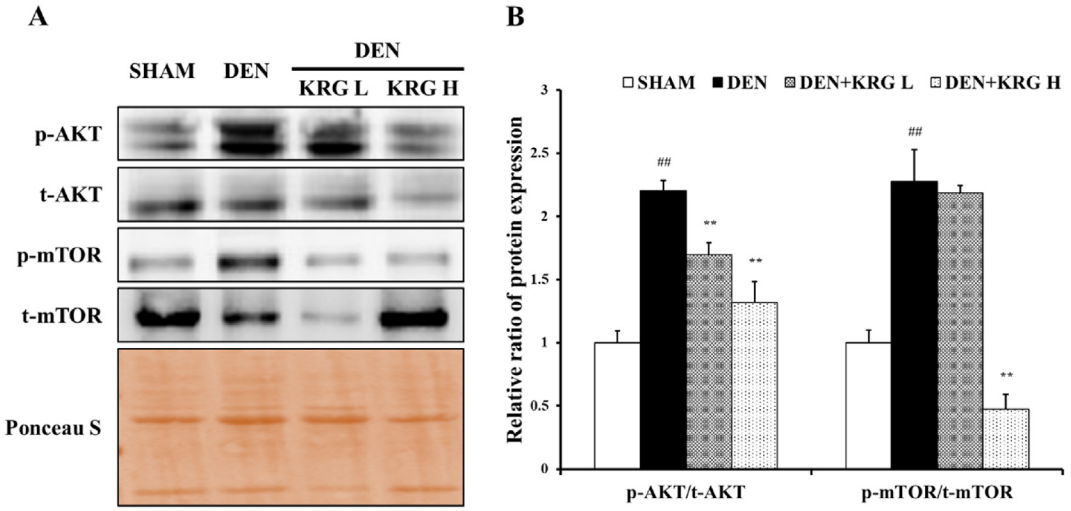

Fig. 4. KRG reduced the elevated phosphorylation of (A) AKT and mTOR. (B) The densitometric values were determined using ChemiDoc. DEN; denervation-induced mice, DEN + KRG L; denervation-induced mice + oral administration of low-dose (100 mg/kg/day) of KRG, DEN + KRG H; denervation-induced mice + oral administration of high-dose (400 mg/kg/day) KRG. Values: means ± SD ($n = 7$). Significance: $^{\#\#}p < 0.01$ vs SHAM; $^{**}p < 0.01$ vs DEN.

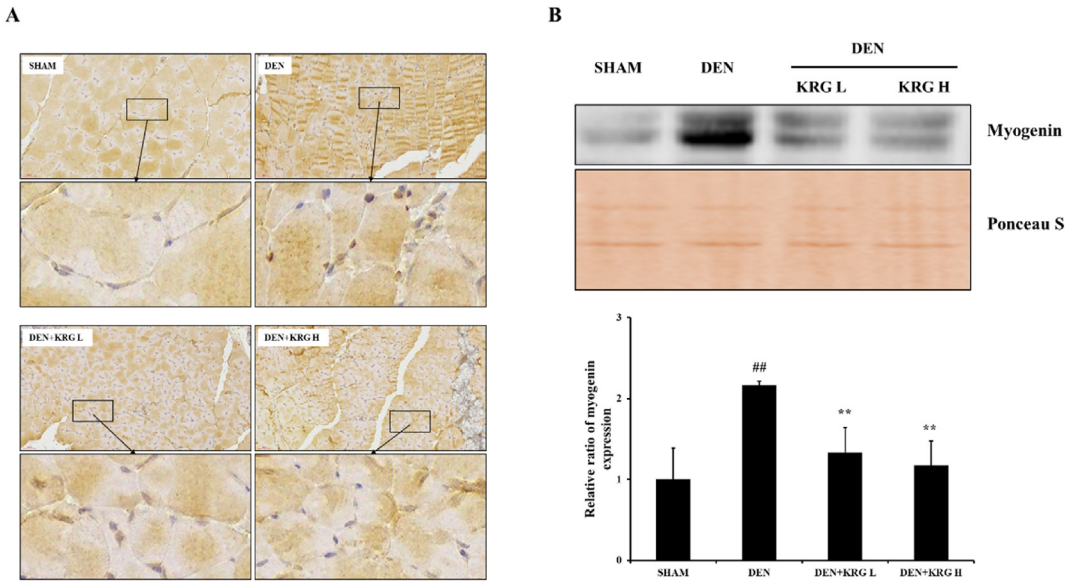

Fig. 5. KRG reduces the elevated (A) myogenin positivity and (B) myogenin expression in TA muscles from mice which was confirmed by IHC and Western blot. DEN; denervation-induced mice, DEN + KRG L; denervation-induced mice + oral administration of low-dose (100 mg/kg/day) of KRG, DEN + KRG H; denervation-induced mice + oral administration of high-dose (400 mg/kg/day) KRG. Values: means ± SD ($n = 7$). Significance: $^{\#\#}p < 0.01$ vs SHAM; $^{**}p < 0.01$ vs DEN.

phosphorylated AKT and mTOR levels compared to the denervation-alone groups.

3.5. Effects of KRG on denervation-induced myogenin expression in the TA muscle

We also investigated the effect of KRG on myogenin expression in denervation-inoculated mice. The denervation-induced mice showed higher myogenin positivity in the TA muscle as revealed by IHC when compared to the sham group (Fig. 5A). However, KRG-treated mice showed decreased myogenin expression level in the TA muscle in a dose proportional pattern. Similarly, increased myogenin expression level, evaluated by Western blot, was evidently diminished in the KRG-treated groups compared to that in the denervation group (Fig. 5B). However, there was no significant difference in myogenin expression level in the denervation + KRG-treated groups compared with that in the denervation-alone group in GA and quad riceps (Supplemental Fig. 1).

4. Discussion

Nerve injury leads to pathologic alterations in the skeletal muscle, such as remodeling of the postsynaptic apparatus and loss of muscle mass [24]. Apoptosis is a crucial contributor to denervation-induced skeletal muscle atrophy [7,25]. In this study, we expected a muscle protective effect of KRG against sciatic nerve dissection based on previous studies that demonstrated the potential beneficial effect of KRG on chemical or immobilization-induced muscle degeneration [26,27]. In this study, we first demonstrated that KRG improved denervation-induced muscle injury by suppressing the p53-mediated apoptotic signal in denervated muscle and decreasing AKT/mTOR signaling, which might indicate damage remission following KRG treatment.

We induced skeletal muscle atrophy by dissecting the sciatic nerves to evaluate the effects of KRG on denervation-induced skeletal muscle atrophy. TA is a faster twitch type II fiber-rich muscle than GA and quadriceps and is vulnerable to stimuli with a higher rate of atrophy than type I fibers under denervation conditions [28–30]. The difference in the impact of denervation between the muscle parts is in line with previous reports. In the present study, TA showed the most evident denervation-induced muscle atrophy among the examined muscles. Moreover, the apoptotic signal induced after denervation was relatively smaller in the GA and quadriceps than in the TA, supporting different sensitivities to denervation stress by muscle type.

Mitochondria-associated apoptotic signaling is activated by decreased muscle mass in denervation-induced skeletal muscle atrophy [8]. p53 directly mediates apoptotic process through translocation to the mitochondria with a transcription-independent mechanism. In addition, increased level of cytoplasmic p53 reported to interact with diverse cytosolic apoptogenic factors including Bax and activate apoptosis during muscle atrophy [9,31]. Reactive oxygen species-mediated oxidative damage is one of the leading theories regarding the mechanisms underlying age-related muscle denervation [32]. Moreover, oxidative stress activates p53-dependent muscle senescence during denervation [33]. The biological role of KRG as an antioxidant has been well demonstrated in previous studies using diverse disease models [34,35]. In the present study, KRG attenuated p53/Bax/cytochrome c/Caspase 3 signaling induced by nerve injury in a dose-dependent manner. Consistent with this result, KRG reduced the number of TUNEL-positive apoptotic cells in the TA muscles.

In the denervated TA muscle, decreased muscle mass was concomitant with a reduction in muscle fiber areas, confirmed by laminin staining analysis. However, KRG treatment prevented skeletal muscle weight loss and improved TA muscle fiber volume in the injured area. Differentiation of skeletal myoblasts is a multistage maturation process forming skeletal myofibers, including the self-renewal of myogenic cells, expression of muscle-specific transcriptional genes, and fusion into multinucleated myofibers [36,37]. Myogenin is a transcription factor that participates in terminal myoblast differentiation and regulates myocyte fusion during development [38]. Myogenin also plays an important role as an essential regulator of myogenesis in regulating denervation-induced atrophy [39]. Myogenin promotes muscle atrophy upon denervation by directly activating the expression of murf-1 and atrogin-1, which encode E3 ubiquitin ligases responsible for muscle protein degradation. Conversely, histone acetylation, which plays an important role in denervation-dependent changes, regulates myogenin expression, and forced expression of myogenin restores muscle atrophy after denervation. Therefore, we focus on myogenin because of its dual role as a regulator of muscle development after denervation-induced atrophy. Myogenin expression was enhanced in the denervation-alone group, presumed to restore muscle atrophy. However, the myogenin expression level in the KRG-treated group was lower than that in the denervation-alone group, at a level similar to that of the sham control group, confirmed by Western blot analysis and IHC. Moreover, the phosphorylation of AKT and mTOR in the KRG-treated group was lower than that in the denervation-alone group, in a dose-dependent manner. The AKT/mTOR pathway plays a major role in muscle hypertrophy [40]. In particular, mTOR has been recognized as the crucial regulator of protein synthesis in muscles under various pathological conditions [41]. In the present study, enhanced AKT phosphorylation in the denervation-alone group was accompanied by enhanced apoptosis-related signals, and KRG treatment reversed this expression pattern. AKT was previously shown to be activated by mitochondrial apoptotic stimuli, and the apoptosis process was delayed by its activation [42]. The overall results indicate that the muscle-improving effect of KRG against denervation-induced muscle atrophy might rely on the inhibition of apoptotic signals that can trigger muscle atrophy and spare the expression of restorative myogenesis activation.

In this study, we investigated the potential protective role of KRG against denervation-induced atrophy. Ameliorated atrophy observed after KRG treatment was accompanied by reduced levels of mitochondria-associated apoptosis. Further detailed evaluations of these molecular events are required to elucidate how KRG sequentially prevents denervation-induced muscle atrophy.

Author contributions

Ji-Soo Jeong prepared the manuscript and performed *in vivo* study, Jeong-Won Kim, Jin-Hwa Kim, and Chang-Yeop Kim carried experimental technical support. Je-Won Ko provided data interpretation and manuscript preparation. Tae-Won Kim conceived the experiments, prepared manuscript, and manage the project. All authors have checked and agreed to the final version of manuscript.

Declaration of competing interest

All authors declare that they have no known competing conflict of interest

Acknowledgements

This work was supported by the National Research Foundation of Korea (NRF) grant funded by the Korean government (MSIT) (2021R1A4A1033078) and the Basic Science Research Program

through the NRF funded by the Ministry of Education (2021R1A6A1A03045495).

Appendix A. Supplementary data

Supplementary data to this article can be found online at https://doi.org/10.1016/j.jgr.2023.07.002.

References

[1] Shirakawa T, Miyawaki A, Kawamoto T, Kokabu S. Natural compounds attenuate denervation-induced skeletal muscle atrophy. Int J Mol Sci 2021;22(15):8310.
[2] Eisenberg HA, Hood DA. Blood flow, mitochondria, and performance in skeletal muscle after denervation and reinnervation. J Appl Physiol 1994;76(2):859–66. 1985.
[3] Wicks KL, Hood DA. Mitochondrial adaptations in denervated muscle: relationship to muscle performance. Am J Physiol 1991;260(4 Pt 1):C841–50.
[4] Jackman RW, Kandarian SC. The molecular basis of skeletal muscle atrophy. Am J Physiol Cell Physiol 2004;287(4):C834–43.
[5] Primeau AJ, Adhihetty PJ, Hood DA. Apoptosis in heart and skeletal muscle. Can J Appl Physiol 2002;27(4):349–95.
[6] Dirks AJ, Leeuwenburgh C. The role of apoptosis in age-related skeletal muscle atrophy. Sports Med 2005;35(6):473–83.
[7] Adhihetty PJ, O'Leary MF, Chabi B, Wicks KL, Hood DA. Effect of denervation on mitochondrially mediated apoptosis in skeletal muscle. J Appl Physiol 1985;102(3):1143–51. 2007.
[8] Memme JM, Oliveira AN, Hood DA. p53 regulates skeletal muscle mitophagy and mitochondrial quality control following denervation-induced muscle disuse. J Biol Chem 2022;298(2):101540.
[9] Siu PM, Alway SE. Mitochondria-associated apoptotic signalling in denervated rat skeletal muscle. J Physiol 2005;565(Pt 1):309–23.
[10] Mahady GB, Gyllenhall C, Fong HH, Farnsworth NR. Ginsengs: a review of safety and efficacy. Nutr Clin Care 2000;3:90–101.
[11] Kim JH. Pharmacological and medical applications of *Panax ginseng* and ginsenosides: a review for use in cardiovascular diseases. J Ginseng Res 2018;42(3):264–9.
[12] Kim JH, Yi YS, Kim MY, Cho JY. Role of ginsenosides, the main active components of *Panax ginseng*, in inflammatory responses and diseases. J Ginseng Res 2017;41(4):435–43.
[13] Ye R, Zhang X, Kong X, Han J, Yang Q, Zhang Y, Chen Y, Li P, Liu J, Shi M, et al. Ginsenoside Rd attenuates mitochondrial dysfunction and sequential apoptosis after transient focal ischemia. Neuroscience 2011;178:169–80.
[14] Jiang GZ, Li JC. Protective effects of ginsenoside Rg1 against colistin sulfate-induced neurotoxicity in PC12 cells. Cell Mol Neurobiol 2014;34(2):167–72.
[15] Liu M, Bai X, Yu S, Zhao W, Qiao J, Liu Y, Zhao D, Wang J, Wang S. Ginsenoside Re inhibits ROS/ASK-1 dependent mitochondrial apoptosis pathway and activation of Nrf2-antioxidant response in beta-amyloid-challenged SH-SY5Y cells. Molecules 2019;24(15):2687.
[16] Huang Q, Gao S, Zhao D, Li X. Review of ginsenosides targeting mitochondrial function to treat multiple disorders: current status and perspectives. J Ginseng Res 2021;45(3):371–9.
[17] Ma YL, Sun YZ, Yang HH. [Protective effect of RenShen compound and DanHuang compound on muscle atrophy in suspended rats]. Space Med Med Eng (Beijing) 1999;12(4):281–3.
[18] Jiang R, Wang M, Shi L, Zhou J, Ma R, Feng K, Chen X, Xu X, Li X, Li T, et al. *Panax ginseng* total protein facilitates recovery from dexamethasone-induced muscle atrophy through the activation of glucose consumption in C2C12 myotubes. Biomed Res Int 2019;2019:3719643.
[19] Li F, Li X, Peng X, Sun L, Jia S, Wang P, Ma S, Zhao H, Yu Q, Huo H. Ginsenoside Rg1 prevents starvation-induced muscle protein degradation via regulation of AKT/mTOR/FoxO signaling in C2C12 myotubes. Exp Ther Med 2017;14(2):1241–7.
[20] Kim JH, Kim JW, Kim CY, Jeong JS, Lim JO, Ko JW, Kim TW. Korean red ginseng ameliorates allergic asthma through reduction of lung inflammation and oxidation. Antioxidants (Basel) 2022;11(8):1422.
[21] Kim JW, Kim CY, Kim JH, Jeong JS, Lim JO, Ko JW, Kim TW. Prophylactic catechin-rich green tea extract treatment ameliorates pathogenic enterotoxic *Escherichia coli*-induced colitis. Pathogens 2021;10(12):1573.
[22] Fortes MA, Marzuca-Nassr GN, Vitzel KF, da Justa Pinheiro CH, Newsholme P, Curi R. Housekeeping proteins: how useful are they in skeletal muscle diabetes studies and muscle hypertrophy models? Anal Biochem 2016;504:38–40.
[23] Nie X, Li C, Hu S, Xue F, Kang YJ, Zhang W. An appropriate loading control for western blot analysis in animal models of myocardial ischemic infarction. Biochem Biophys Rep 2017;12:108–13.
[24] Castets P, Rion N, Théodore M, Falcetta D, Lin S, Reischl M, Wild F, Guérard L, Eickhorst C, Brockhoff M, et al. mTORC1 and PKB/Akt control the muscle response to denervation by regulating autophagy and HDAC4. Nat Commun 2019;10(1):3187.
[25] Siu PM, Pistilli EE, Alway SE. Apoptotic responses to hindlimb suspension in gastrocnemius muscles from young adult and aged rats. Am J Physiol Regul Integr Comp Physiol 2005;289(4):R1015–26.
[26] Babiker LB, Gadkariem EA, Alashban RM, Aljohar HI. Investigation of stability of Korean ginseng in herbal drug product. Am. J. Appl 2014;11:160–70.
[27] Shin EJ, Jo S, Choi S, Cho CW, Lim WC, Hong HD, Lim TG, Jang YJ, Jang M, Byun S, et al. Red ginseng improves exercise endurance by promoting mitochondrial biogenesis and myoblast differentiation. Molecules 2020;25(4):865.
[28] Wang Y, Pessin JE. Mechanisms for fiber-type specificity of skeletal muscle atrophy. Curr Opin Clin Nutr Metab Care 2013;16(3):243–50.
[29] Ika PY, Triadi DA, Herawati L. Non-invasive method on slow-twitch quadriceps muscle fibers dominate a high level of fitness. In: Proceedings of Surabaya International Physiology Seminar; 2017. p. 182–5.
[30] Giacomello E, Crea E, Torelli L, Bergamo A, Reggiani C, Sava G, Toniolo L. Age dependent modification of the metabolic profile of the tibialis anterior muscle fibers in C57BL/6J mice. Int J Mol Sci 2020;21(11):3923.
[31] Siu PM, Alway SE. Id2 and p53 participate in apoptosis during unloading-induced muscle atrophy. Am J Physiol Cell Physiol 2005;288(5):C1058–73.
[32] Salmon AB, Richardson A, Pérez VI. Update on the oxidative stress theory of aging: does oxidative stress play a role in aging or healthy aging? Free Radic Biol Med 2010;48(5):642–55.
[33] Xiang Y, You Z, Huang X, Dai J, Zhang J, Nie S, Xu L, Jiang J, Xu J. Oxidative stress-induced premature senescence and aggravated denervated skeletal muscular atrophy by regulating progerin-p53 interaction. Skelet Muscle 2022;12(1):19.
[34] Ban JY, Kang SW, Lee JS, Chung JH, Ko YG, Choi HS. Korean red ginseng protects against neuronal damage induced by transient focal ischemia in rats. Exp Ther Med 2012;3(4):693–8.
[35] Lee YM, Yoon H, Park HM, Song BC, Yeum KJ. Implications of red *Panax ginseng* in oxidative stress associated chronic diseases. J Ginseng Res 2017;41(2):113–9.
[36] Horsley V, Pavlath GK. Forming a multinucleated cell: molecules that regulate myoblast fusion. Cells Tissues Organs 2004;176(1–3):67–78.
[37] Krauss RS. Regulation of promyogenic signal transduction by cell-cell contact and adhesion. Exp Cell Res 2010;316(18):3042–9.
[38] Schmidt M, Schüler SC, Hüttner SS, von Eyss B, von Maltzahn J. Adult stem cells at work: regenerating skeletal muscle. Cell Mol Life Sci 2019;76(13):2559–70.
[39] Moresi V, Williams AH, Meadows E, Flynn JM, Potthoff MJ, McAnally J, Shelton JM, Backs J, Klein WH, Richardson JA, et al. Myogenin and class II HDACs control neurogenic muscle atrophy by inducing E3 ubiquitin ligases. Cell 2010;143(1):35–45.
[40] Bodine SC, Stitt TN, Gonzalez M, Kline WO, Stover GL, Bauerlein R, Zlotchenko E, Scrimgeour A, Lawrence JC, Glass DJ, et al. Akt/mTOR pathway is a crucial regulator of skeletal muscle hypertrophy and can prevent muscle atrophy *in vivo*. Nat Cell Biol 2001;3(11):1014–9.
[41] Yoon MS. mTOR as a key regulator in maintaining skeletal muscle mass. Front Physiol 2017;8:788.
[42] Tang D, Okada H, Ruland J, Liu L, Stambolic V, Mak TW, Ingram AJ. Akt is activated in response to an apoptotic signal. J Biol Chem 2001;276(32):30461–6.